Journal of the Geological Society, London, Vol. **169**, 2012, pp. 123–126. doi: 10.1144/0016-76492011-108.

SPECIAL

Soft faults with hard tips: magnitude-order displacement gradient variations controlled by strain softening versus hardening; implications for fault scaling

ATLE ROTEVATN[1,2*] & HAAKON FOSSEN[1,2]

[1]*Department of Earth Science, University of Bergen, Allégaten 41, 5007 Bergen, Norway*

[2]*Uni CIPR, University of Bergen, Allégaten 41, 5007 Bergen, Norway*

**Corresponding author (e-mail: atle.rotevatn@uni.no)*

We document magnitude-order displacement gradient variations along single faults as a function of microstructural style, hardening or weakening behaviour during deformation, and the variability of the former two over time during fault evolution in porous sandstone. The observed variations imply that the power-law displacement–length (*D*–*L*) scaling relation, $D_{max}=\gamma L^n$, changes through time and stages of fault evolution. Findings of this study combined with published *D*–*L* data suggest that faults in porous rocks follow a three-stage evolution in *D*–*L* space: (1) proto-fault evolution with $n\sim0.5$; (2) onset of macroscopic discrete slip with *n* in the range of 2–5; (3) stable growth with $n\sim1.0$. This implies that the power-law exponent *n* depends on the maturity of the fault population *D* and the range of fault sizes under consideration. Thus, the relationship between displacement and length is more complicated than previously thought.

Fundamental generic descriptions of fault attribute interdependence, such as relationships between fault length, width and displacement, commonly take the shape of fault scaling laws. It is widely recognized, however, that magnitude-order variability exists in these relations as a function of various geological conditions such as host rock composition and competence, tectonic regime, local and regional stress field, porosity, mechanical properties, strain rate and influence of pre-existing structures (e.g. Dawers *et al*. 1993; Ackermann *et al*. 2001; Walsh *et al*. 2002; Kim & Sanderson 2005; Childs *et al*. 2009). Even so, fault scaling laws and the often-cited relations between fault length, thickness and displacement are commonly based on global fault databases (e.g. Marrett & Allmendinger 1991). Although this approach may provide magnitude-order constraints on possible outcomes of one (unknown) fault attribute based on another (known), trends in more specific datasets may be difficult to discern (e.g. Cowie & Scholz 1992). None the less, there is broad consensus that empirically derived scaling relations based on more specific datasets represent a meaningful tool to understand fault dimensions (e.g. Schultz *et al*. 2008). However, as we will demonstrate in this study, significant and systematic variability in fault scaling behaviour may be seen also within restricted fault populations (herein restricted to faults in porous sandstone).

Displacement, being the benchmark fault attribute toward which all other fault attributes are generally calibrated and compared, is of great importance to fault scaling laws. We here demonstrate that magnitude-order variations in displacement gradients take place even over the length of a single fault, and that processes near the fault tip play an important role in controlling this variability. We do so by investigating the relationship between displacement gradient variations, microstructure, slip accommodation mechanisms and the mechanical response of the host rock to kinematics (strain hardening v. strain softening) in porous rocks. The aim of the study is threefold: (1) to use field data to document magnitude-order differences in displacement gradients along a single fault; (2) to show that these differences are controlled by microstructural slip accommodation mechanisms and strain hardening or softening processes; (3) by combining data presented herein with data from the published literature, to demonstrate that this has significant implications for the understanding of fault scaling relations in porous sandstones.

Terminology. For clarity we describe the terminology used here for the studied structural features. We use the term fault to describe the complete structural entity, including the fault core, damage zone, process zone and the main fault surface(s). The fault core defines the rock volume where the majority of the displacement is accommodated, and where the main fault surface(s) and highly strained fault rocks are localized. The damage zone, enveloping the fault core and having accommodated a minority of the displacement, is typically characterized by fractures, deformation bands and slip surface patches. The process zone (*sensu* Cowie & Shipton 1998) is the part of the damage zone that extends past the tip point (tip line in three dimensions) of the main fault surface itself. We treat fault length as the total length of the entire fault envelope, including both the discrete fault surface and the process zone.

Background, framework and methods. Faulting in porous siliciclastic rocks is fundamentally different from faulting in non-porous rocks (Aydin & Johnson 1978). Available pore space allows the formation of strain localization features known as deformation bands (Aydin 1978), notably compactional shear bands. Such bands (hereafter referred to as deformation bands) form as a result of shear through grain reorganization with additional compaction, and may or may not involve grain crushing. Aydin & Johnson (1978) realized that faulting in porous sandstones is characterized by sequential development of deformation band into swarms and clusters. Eventually slip surfaces nucleate, grow and amalgamate into a through-going, continuous slip surface along which larger offsets are accumulated (Shipton & Cowie 2001). A consequence of this model is that the formation of damage zones and process zones (proto-fault) in porous sandstones precedes the development of the discrete fault itself.

Previous workers (e.g. Cowie & Shipton 1998) have shown that in porous sandstones, discrete displacement (i.e. along a fault surface) exhibits an approximately linear decay toward the tip. What has been less well studied is how displacement accommodated by minor structures in the damage zone and process zone contribute to the total displacement distribution. To investigate this we have studied the extremely well-exposed tip region of a *c*. 3 km long

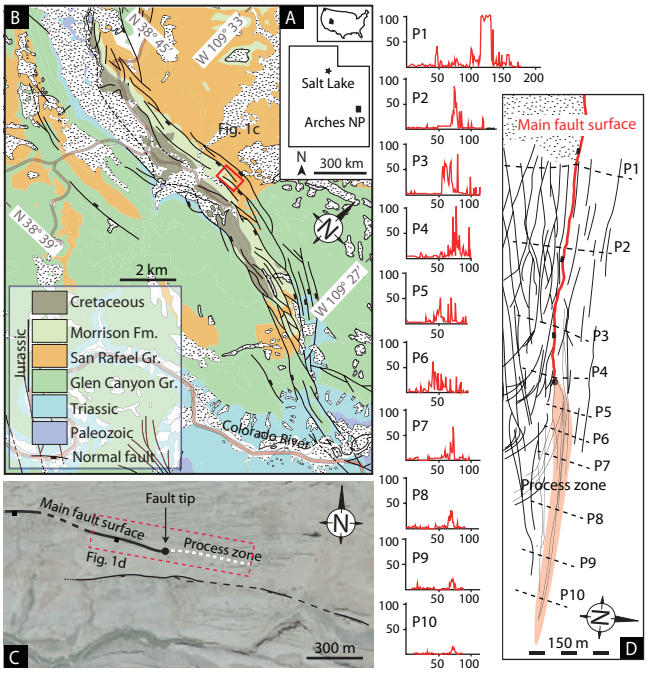

Fig. 1. (**a**) Location of Arches National Park (NP) in Utah, USA. (**b**) Geological map of Arches NP (modified from Antonellini & Aydin 1995; Doelling 2001). (**c**) Aerial photography of the study area; the fault and process zone analysed in (**d**) is outlined (red box). (**d**) Structural map showing the main fault and major deformation band trends; the process zone is highlighted in red shade (grey in printed version). Profiles P1–P4 record structural intensity across the damage zone and main fault; profiles P5–P10 record structural intensity across the process zone. Horizontal axes show length along profiles from south to north; vertical axes show deformation bands per metre. (Note that the direction of north varies between figures.)

normal fault forming part of an east–west-trending extensional fault array following the collapsed crest of the Salt Valley salt wall in Arches National Park, SE Utah, USA (Fig. 1). The fault dissects beds of the well-sorted, highly porous aeolian Entrada sandstone of the Jurassic San Rafael Group. Displacement in the tip region was mapped in detail; *c*. 400 m westward along strike from the tip point along the main fault surface and *c*. 400 m eastward past the tip point along the process zone (Fig. 1c and d). Measurable displacement along the main fault surface was recorded using the top of the Slickrock Member of the Entrada Formation as a marker surface. Displacement accommodated by deformation bands was recorded cumulatively, combining average displacement per deformation band (2 mm) and measured deformation band frequency along north–south scan lines (Fig. 1d) across the core, damage zone and process zone.

Field data and results: along-strike distribution of fault displacement and width. The studied fault exhibits a core of cataclasite, clusters of cataclastic deformation bands with centimetre-scale host rock lenses, and discrete slip surfaces. The scan lines all exhibit structural frequency maxima representing the damage zone (Fig. 1d, profiles P1–P4) and the process zone (Fig. 1d, profiles P5–P10). The maxima decrease progressively toward the end of the damage zone and process zone going east. The damage zone is characterized by anastomosing single and clusters of deformation bands. The process zone is fully exposed and features deformation bands and clusters that are continuous for up to 400 m past the fault tip (Fig. 1d).

The displacement data (Fig. 2a) show that along the main fault surface, discrete slip accounts for the majority of displacement whereas accumulated millimetre-scale shear within deformation bands in the damage zone accounts for a minor component. Displacement in the process zone is accommodated exclusively by deformation bands. The data clearly show near-linear displacement decay toward the fault tip of *c*. 0.1, within the upper range of previously reported displacement gradient values (e.g. Walsh & Watterson 1989), reflecting interaction with the fault immediately to the south (Fig. 1c). An abrupt change in the displacement gradient is seen into the process zone, where displacement decays at a rate of *c*. −0.003. This represents a displacement gradient contrast of nearly two orders of magnitude at the fault tip.

Total damage/process zone width (using 10 deformation bands per metre as the damage/process zone cut-off) was recorded along strike of the fault system (Fig. 2b). The dataset exhibits two peaks that deviate from the otherwise semi-linear decay toward the end of the process zone. The peaks are associated with two segment overlap zones that are hard-linked and soft-linked, respectively.

The displacement–width (*D–W*) ratio (where displacement equals total displacement as recorded in Figure 2a and width represents damage–process zone width as shown in Fig. 2b) shows large variability along the length of the fault system (Fig. 2c). Along the main fault surface, the *D–W* ratio varies mainly between 0.4 and 0.8, although extremes of 0.2 and 1.3 were recorded. In the process zone, the *D–W* ratio ranges between *c*. 0.02 and 0.05 in the process zone, an order of magnitude less than that of the damage zone along the main fault surface.

Discussion. Three chief mechanisms are suggested as being jointly responsible for the magnitude-order displacement gradient variability observed in the current study: (1) microstructural slip accommodation mechanisms (failure mode); (2) the mechanical response of the host rock to kinematics (strain hardening v. strain softening); (3) the variability of the former two over time during fault evolution in porous sandstone.

Initial stages of fault evolution in porous sandstones are associated with sequential development of single and clusters of cataclastic deformation bands (e.g. Aydin & Johnson 1978). Microstructurally this translates to a combination of granular flow and brittle grain crushing. The resulting tighter grain packing arrangement and enhanced grain angularity lead to increased shear resistance (Mair *et al*. 2002). The critical stress condition required for repeated failure or continued yield thus increases, which is essentially a strain hardening behaviour (Baud *et al*. 2006). This strain hardening stage characterizes the process zone and is responsible for the low-magnitude displacement recorded along this part of the fault (Fig. 3, stages A and B).

Subsequently, discrete slip surface nucleation and growth (processes that characterize the fault tip; Fig. 3, stage C) occur when some sections of a strain hardened network of deformation bands eventually achieve the critical stress state associated with frictional sliding (Schultz & Siddharthan 2005). From this point on, patches of discrete slip surfaces may nucleate, grow and amalgamate until they coalesce into a through-going fault plane (Fig. 3, stage D). Microstructurally, slip surfaces are thin zones of ultracataclasite that accommodate strain without an appreciable amount of additional grain crushing (Shipton & Cowie 2001). Discrete slip surfaces are therefore low-friction or 'soft' features, associated with cohesion loss and weakening during failure.

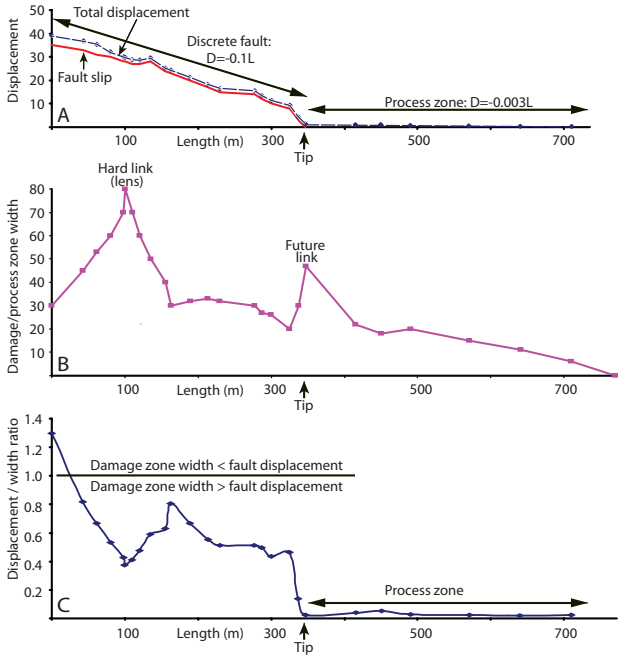

Fig. 2. Distribution of selected fault attributes along the length of the main fault and process zone. (**a**) Displacement; discrete displacement along main fault surface (red) and cumulative displacement recorded by deformation bands (blue) are shown. (**b**) Damage/process zone width. (**c**) *D:W* ratio (displacement:damage/process zone width).

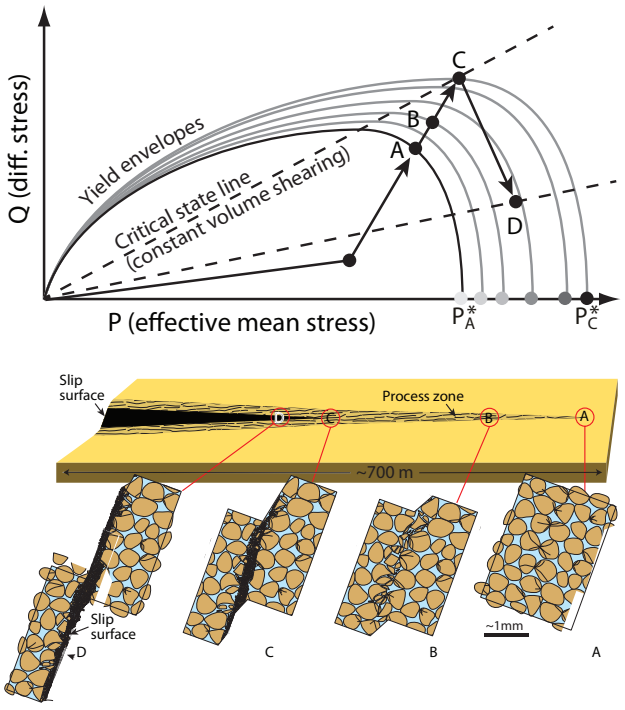

Fig. 3. Different stages (A–D) of fault evolution in porous rocks may be recognized along a single fault as in this study, here shown in three panels. Upper panel: *Q–P* diagram (differential stress v. mean stress) applied to porous rocks; *P** is the grain crushing pressure at different stages; strain hardening in stages A–C is reflected by progressive enlargement of the yield envelope (adapted from Schultz & Siddharthan 2005). Middle panel: 3D model of the studied fault. Lower panel: microstructural processes at each stage.

The two interacting failure regimes appear to control slip magnitude and distribution in evolving fault zones in porous sandstones: first, the initial strain hardening regime (Fig. 3, stages A and B), where grain crushing and the development of cataclastic deformation bands allows only millimetre- to centimetre-scale displacement to occur (development of the incipient fault zone, a precursory damage and process zone); second, the strain softening regime (Fig. 3, stages C and D), where frictional sliding and the development of discrete slip surfaces (eventually a through-going slip plane), prone to reactivation, accommodates macroscopic displacement (metre to kilometre scale).

The observed magnitude-order displacement gradient variability is therefore tied to microstructural deformation mechanisms, strengthening or weakening behaviour of the fault zone, and the temporal evolution of the fault zone: macroscopic displacement recorded along the 'soft', discrete fault plane yields displacement gradients two orders of magnitude higher than that of the 'hard' process zone where only millimetre-scale shear is accommodated.

The staged evolution of faults in porous sandstones, where the growth of the proto-fault of deformation band clusters precedes the main fault surface, also explains the non-abrupt near-linear decay of the damage zone width into the process zone (Fig. 2b): the width at the tip of the main fault surface represents the width of the proto-fault zone at the time of rupture (Shipton & Cowie 2001).

Implications for displacement–length (*D–L*) scaling. Maximum displacement D_{max} and horizontal length L are related by $D_{max}=\gamma L^n$, n generally being close to 1.0 for general fault populations (Fig. 4a) and 0.5 for deformation bands (Fig. 4b). Here γ is a proportionality constant. Relating total fault length to displacement is less than straightforward in porous sandstone, as indicated by the magnitude-order displacement gradient variations observed in the current study. Furthermore, the temporal relation where the process zone precedes the mother fault has important implications for fault scaling relations: the establishment and growth of a damage zone envelope prior to slip plane development suggests that the incipient zone must reach a critical size before macroscopic brittle shear failure occurs. The process zone may be hundreds of metres of length prior to rupture as suggested by previous findings in the Navajo Sandstone (Shipton & Cowie 2001) and supported by the current study. Cowie & Shipton (1998) argued that process zone length does not scale with total fault slip surface length, indicating that faults of any length in a given lithology will have roughly the same size (width and length) process zone. This has significant ramifications for the scalability of displacement to total fault length, as faults with short slip surfaces and low displacement maxima will have disproportionately long total fault lengths. It also affects the scaling relations of small faults (early stage, short slip surfaces) compared with large faults (later stage, long slip surfaces). In general, this model predicts that faults in porous sandstones will have different *D–L* scaling relations during different stages in their evolution. Based on the findings presented herein and published scaling data (Fig. 4a and b) we propose the following evolution in *D–L* space for faults in porous sandstone (Fig. 4c): (1) in the proto-fault domain during deformation band cluster growth, (proto)-faults will scale as deformation bands with n in the range of 0.5; (2) when the proto-fault reaches it critical length and discrete slip initiates, displacement rapidly increases, upon which the *D–L* relation will follow a significantly steeper trend (n in the range of 2–5) for a period. Eventually, (3) when total fault length becomes orders of magnitude greater than the process zone length, the fault will scale as other faults with n in the range of 1.0.

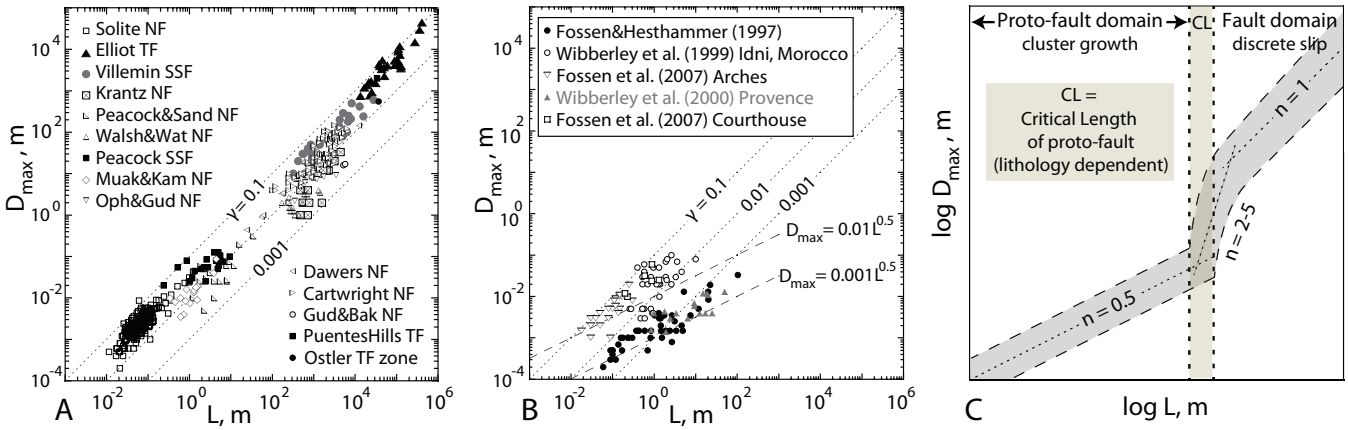

Fig. 4. D_{max}–L distributions. (**a**) Compilation of faults (for sources of data and discussion see Schultz *et al*. 2008, and references therein). Open symbols, normal faults (NF); grey symbols, strike-slip faults (SSF); filled symbols, thrust faults (TF). Lines of constant slope are shown: $n = 1$, dotted, with $D/L = \gamma$. (**b**) Compilation of deformation bands (for discussion see Schultz *et al*. 2008, and references therein). Filled circles and triangles, cataclastic bands; open symbols, isochoric shear bands. Lines as in (**a**). Data sources: Fossen & Hesthammer (1997); Wibberley *et al*. (1999, 2000); Fossen *et al*. (2007). (**c**) Idealized D_{max}–L distribution for faults in porous sandstones. Lines of constant slope are shown (dotted) for different segments of the distribution; $n = 0.5$, $n = 2$–5, $n = 1.0$.

Summary and conclusions. We have documented magnitude-order displacement gradient variations along a single fault as a function of microstructural style, hardening or weakening behaviour during deformation, and the variability of the former two during fault growth in porous sandstone. The observed variability implies that the D–L scaling relation changes through time and stages of fault evolution (Fig. 4c). Further to contributing toward an increased understanding of a dynamic D–L relation, implications include better estimation of total lengths of faults from subsurface displacement data (seismic, well), significant portions of which will be below vertical seismic resolution.

The US National Park Service is acknowledged for permission to work inside Arches National Park. Reviewer T. Needham and Subject Editor K. McCaffrey are thanked for their helpful and constructive comments. E. Bastesen is thanked for discussions and critical feedback.

References

Ackermann, R.V., Schlische, R.W. & Withjack, M.O. 2001. The geometric and statistical evolution of normal fault systems: an experimental study of the effects of mechanical layer thickness on scaling laws. *Journal of Structural Geology*, **23**, 1803–1819.

Antonellini, M. & Aydin, A. 1995. Effect of faulting on fluid flow in porous sandstones: geometry and spatial distribution. *AAPG Bulletin*, **79**, 642–671.

Aydin, A. 1978. Small faults formed as deformation bands in sandstone. *Pageoph*, **116**, 913–930.

Aydin, A. & Johnson, A.M. 1978. Development of faults as zones of deformation bands and as slip surfaces in sandstone. *Pageoph*, **116**, 931–942.

Baud, P., Vajdova, V. & Wong, T.-F. 2006. Shear-enhanced compaction and strain localization: inelastic deformation and constitutive modeling of four porous sandstones. *Journal of Geophysical Research*, **111**, doi:10.1029/2005JB004101.

Childs, C., Manzocchi, T., Walsh, J.J., Bonson, C.G., Nicol, A. & Schöpfer, M.P.J. 2009. A geometric model of fault zone and fault rock thickness variations. *Journal of Structural Geology*, **31**, 117–127.

Cowie, P.A. & Scholz, C.H. 1992. Displacement–length scaling relationship for faults: data synthesis and discussion. *Journal of Structural Geology*, **14**, 1149–1156.

Cowie, P.A. & Shipton, Z.K. 1998. Fault tip displacement gradients and process zone dimensions. *Journal of Structural Geology*, **20**, 983–997.

Dawers, N.H., Anders, M.H. & Scholz, C.H. 1993. Growth of normal faults: displacement–length scaling. *Geology*, **21**, 1107–1110.

Doelling, H.H. 2001. *Geologic map of the Moab and eastern part of the San Rafael Desert 30' × 60' quadrangles, Grand and Emery Counties, Utah, and Mesa County, Colorado*. Utah Geological Survey Map, **180**.

Fossen, H. & Hesthammer, J. 1997. Geometric analysis and scaling relations of deformation bands in porous sandstone from the San Rafael Desert, Utah. *Journal of Structural Geology*, **19**, 1479–1493.

Fossen, H., Schultz, R., Shipton, Z. & Mair, K. 2007. Deformation bands in sandstone – a review. *Journal of the Geological Society, London*, **164**, 755–769.

Kim, Y.-S. & Sanderson, D.J. 2005. The relationship between displacement and length of faults: a review. *Earth-Science Reviews*, **68**, 317–334.

Mair, K., Frye, K.M. & Marone, C. 2002. Influence of grain characteristics on the friction of granular shear zones. *Journal of Geophysical Research*, **107**, doi:10.1029/2001JB000516.

Marrett, R. & Allmendinger, R.W. 1991. Estimates of strain due to brittle faulting: sampling of fault populations. *Journal of Structural Geology*, **13**, 735–738.

Schultz, R.A. & Siddharthan, R. 2005. A general framework for the occurrence and faulting of deformation bands in porous granular rocks. *Tectonophysics*, **411**, 1–18.

Schultz, R.A., Soliva, R., Fossen, H., Okubo, C.H. & Reeves, D.M. 2008. Dependence of displacement–length scaling relations for fractures and deformation bands on the volumetric changes across them. *Journal of Structural Geology*, **30**, 1405–1411.

Shipton, Z.K. & Cowie, P.A. 2001. Damage zone and slip surface evolution over μm to km scales in high-porosity Navajo sandstone, Utah. *Journal of Structural Geology*, **23**, 1825–1844.

Walsh, J.J. & Watterson, J. 1989. Displacement gradients on fault surfaces. *Journal of Structural Geology*, **11**, 307–316.

Walsh, J.J., Nicol, A. & Childs, C. 2002. An alternative model for the growth of faults. *Journal of Structural Geology*, **24**, 1669–1675.

Wibberley, C.A.J., Petit, J.-P. & Rives, T. 1999. Mechanics of high displacement gradient faulting prior to lithification. *Journal of Structural Geology*, **21**, 251–257.

Wibberley, C.A.J., Petit, J.-P. & Rives, T. 2000. Mechanics of cataclastic 'deformation band' faulting in high-porosity sandstone, Provence. *Comptes Rendus de l'Academie des Sciences, Series IIA*, **331**, 419–425.

Received 2 September 2011; revised typescript accepted 15 December 2011.

Scientific Editing by Ken McCaffrey.